ELSEVIER

Chemical Geology 160 (1999) 39–62

CHEMICAL GEOLOGY
INCLUDING
ISOTOPE GEOSCIENCE

Initial and long-term dissolution rates of aluminosilicate glasses enriched with Ti, Zr and Nd

G. Leturcq [a,b,*], G. Berger [b], T. Advocat [a], E. Vernaz [a]

[a] *Commissariat à l'Energie Atomique (CEA), Valrhô DCC / DRRV / SCD, BP 171, 30207 Bagnols-sur-Cèze Cedex, France*
[b] *Université Paul Sabatier, CNRS, UMR 5563, 38 rue des 36 Ponts, 31400 Toulouse, France*

Received 23 February 1998; received in revised form 9 March 1999; accepted 9 March 1999

Abstract

The alteration mechanism and rate of three aluminosilicate glasses were investigated experimentally in aqueous media between 90 and 200°C. In order to assess their containment properties with regard to minor actinides for the purpose of developing new radionuclide containment matrices, the three glasses were enriched with neodymium to simulate the trivalent actinides. The proportions of the major glass network formers, silicon and aluminum, were comparable to those found in tholeitic basalt glasses. The composition differences for the other elements (Ca, Zr, Ti, Nd) revealed the role of glass network modifiers in aqueous corrosion resistance of silicate glasses. Two types of experiments were performed: open-system leaching to determine the dissolution rate constants at 90, 150 and 200°C; and closed-system tests at high (200 cm^{-1}) SA/V ratios (glass-surface-area-to-leaching-solution-volume) for 3 months at 90°C to simulate long-term behavior. The open-system test results showed that, regardless of the aluminosilicate glass composition (not only the test glasses, but also tholeitic basalt glasses and nuclear aluminoborosilicate glasses), the initial dissolution rates are on the same order of magnitude in neutral or slightly basic media, with a common activation energy of 60 ± 5 kJ mol^{-1}. This step appears to be controlled exclusively by hydrolysis of the Si–O and/or Al–O bonds, irrespective of the nature of the network modifying or intermediate components. Otherwise, with renewal of the leaching solution, the formation of alteration films at the 'glass/solution' interface appears to limit glass alteration; however, the protective effect of these layers depends on the experimental conditions and on the glass composition. Finally, in closed-system conditions studied at 90°C, the three test glasses exhibit very low alteration rates (three to four orders of magnitude lower than the initial rates) without the development of a thick and abundant altered layer. Two hypotheses are discussed to account for these low rates: a protective aluminosilicate surface gel less than 50 nm thick and thus with a low silicon diffusion coefficient ($\sim 10^{-13}$ cm^2 s^{-1}); and a chemical affinity effect with respect to the glass itself, as the solubility products attributed to glass are determined from the thermodynamic model proposed by Paul (1977) [Paul, A., 1977. Chemical durability of glasses: a thermodynamic approach. J. Mater. Sci. 12, 2246–2268.].

Keywords: Sphene glass; Zirconolite glass; SiAlON glass; Basaltic glass; Dissolution kinetics; Reaction affinity

1. Introduction

The issue of high-level nuclear waste containment by vitrification at industrial scale has given rise to

* Corresponding author. Commissariat à l'Energie Atomique (CEA), Valrhô DCC/DRRV/SCD, BP 171, 30207 Bagnols-sur-Cèze Cedex, France. fax: +33-46679-6620; e-mail: gilles.leturcq@cea.fr

0009-2541/99/$ - see front matter
PII: S0009-2541(99)00055-8

many experimental investigations on the alteration of aluminoborosilicate glasses (e.g., Noguès, 1984; Fillet, 1987; Lutze and Ewing, 1988; Tovena, 1995). The mechanisms and kinetic laws established to date from laboratory studies are based on the concept of hydrolysis of the glass network, comprising former, intermediate and modifier oxides as defined by Zachariasen (1932). Guy and Schott (1989) showed that the initial dissolution rate of a basalt glass depends on all the network formers; Advocat et al. (1993) also emphasized the importance of modifier oxides in determining the initial rates of borosilicate glasses. The kinetic role of aqueous species has been addressed in other studies, notably by Grambow (1987), who showed that the dissolution rate of a borosilicate glass was dependent on the silica concentration in solution. These observations spurred several investigations of the nature of the activated complex involved in silicate glass dissolution. Grambow (1987) suggested that the dissolution of aluminoborosilicate glass is controlled by hydrolysis of silica, and also introduced the notion of a residual chemical affinity at silica saturation. Berger et al. (1994), working with basaltic glass, postulated an activated complex for each network former (Si, Al), with the overall glass dissolution rate resulting from competition among the elementary reactions. This was consistent with the kinetic concepts advanced by Chou and Wollast (1985) and by Holdren and Speyer (1985) for aluminosilicate minerals. The joint role of aluminum and silicon was also cited by Gin (1996) to describe the alteration kinetics of an aluminoborosilicate glass (called R7T7) devoted to immobilize fission product solutions. Daux et al. (1997) also proposed a mechanism involving a single activated complex composed of the glass network formers (Si, Al and Fe for basaltic glass).

Kinetic control of glass alteration by secondary phases has also been investigated. Some authors have shown that under certain conditions, a protective gel is formed, either from the residual hydrated glass skeleton (Vernaz and Dussossoy, 1992, for R7T7 glass; Berger et al., 1994, for basalt glass) or from products precipitated on the glass surface (Guy, 1989; Abrajano et al., 1990; Trotignon, 1990; Jollivet, 1996).

However, most of these studies have concentrated mainly on tholeitic basalt glass and nuclear aluminoborosilicate glasses. The dissolution of glasses with very different chemical compositions must be considered to assess the relative importance of the network formers and modifiers.

The work presented here is part of a research program on developing new containment matrices specifically for the high-level radionuclides found in radioactive wastes. The candidate materials will be assessed on the basis of their containment properties for the minor actinides (Pu, Np, Am, Cm) simulated in this study by neodymium. This study also provides information concerning possible silicate glass compositions with greater resistance to alteration than those currently known. A particular area of interest is the possible role of scarcely soluble heavy elements (Ti, Zr and the rare earths).

Three glasses containing the same network former oxides (SiO_2 and Al_2O_3) were tested: a SiAlON glass containing Si, Al, N and Nd (nitrogen was used here as a corrosion tracer), and two glassy precursors of glass ceramics (a mixture of crystals and residual glasses) obtained after heat treatment (Reimann and Kong, 1993; Fillet et al., 1998): a sphene-based glass composition containing Si, Al, Ca, Ti and Nd, and a zirconolite-based glass composition containing Si, Al, Ca, Zr, Ti and Nd. The 2 glassy precursors do not have the compositions of the sphene and zirconolite phases; Nevertheless, the terminology is kept for convenience.

Two types of experiments were conducted. The initial glass dissolution rates were measured at 90, 150 and 200°C using a flow-through reactor to impose and maintain a constant chemical reaction affinity. Additional experiments were conducted in a closed system at 90°C to simulate long-term alteration.

2. Methods

2.1. Initial materials

The nitride glass was fabricated in a dry box to avoid oxidation. Ten-gram batches of reagent grade oxides and AlN were melted at 1480°C in a molybdenum crucible (Rocherullé et al., 1989). No crystallized phases were identified by X-ray diffraction analysis. The chemical composition (Table 1) was determined by acid and lithium tetraborate etching.

Table 1
Chemical composition of the initial glasses and log K (90°C) for dissolution of 1 mole of the various oxides

Species	SiO_2	Al_2O_3	CaO	TiO_2	Nd_2O_3	ZrO_2	N
Analyzed (wt.%)							
Sphene	40.71	11.98	19.7	12.5	15.11	–	–
Zirconolite	40.75	12	19.72	12.51	6.52	8.5	–
SiAlON	32.3	11.4	–	–	53.8	–	1.65
Calculated (mol%)							
Sphene	50.28	8.72	26.06	11.61	3.33	–	–
Zirconolite	48.71	8.45	25.25	11.25	1.39	4.95	–

Oxide dissolution reactions	log K (90°C)	References
$SiO_2 + 2H_2O \rightleftarrows H_4SiO_4$	−2.97	Phillips et al., 1988
$Al_2O_3 + 5H_2O \rightleftarrows 2Al(OH)_4^- + 2H^+$	−22.08	Phillips et al., 1988
$CaO + 2H^+ \rightleftarrows Ca^{2+} + H_2O$	26.54	Cox et al., 1989
$TiO_2 + 3H_2O \rightleftarrows Ti(OH)_5^- + H^+$	−14.16	Cox et al., 1989
$Nd_2O_3 + 3H_2O \rightleftarrows 2Nd(OH)_3$	−91.9	Wagman et al., 1982
$ZrO_2 + 3H_2O \rightleftarrows Zr(OH)_5^- + H^+$	−7.32	Allard and Beall, 1978; Chase et al., 1985

The nitrogen content of the SiAlON glass was measured with a LECO O_2–N_2 analyzer. The glass samples were reduced to sized particles (125–250 μm and 40–50 μm) by grinding and screening, and then ultrasonically cleaned in deionized water to eliminate the ultrafine particles produced by grinding. The specific surface area of each fraction was determined by BET methods using krypton as the adsorbate gas, and is indicated in Table 2 together with the relative density as determined by hydrostatic measurements.

2.2. Experimental procedure

2.2.1. Open-system experiments

The dissolution rates for the three glass compositions were measured in deionized water at 90, 150 and 200°C. The SiAlON glass dissolution rates were also measured at the same three temperatures in sodium sulfate solutions (0.01 M and 0.1 M). These additional leach tests on the SiAlON glass, in Na_2SO_4 enriched solutions, were conducted to increase the Nd solubility in water by complexation with the sulfate ions. The idea was then to avoid the precipitation of a Nd enriched surface layer, able to control the kinetics of dissolution of the sound glass by a protective effect.

Table 2
Specific surface area (g m^{-2}) and density of the starting glasses

Species	Specific surface area (m^2 g^{-1})		Relative density
	40–50 μm	125–250 μm	
Sphene	0.106	0.030	3.14
Zirconolite	0.099	0.025	3.04
SiAlON	0.094	0.028	3.81

The experiments were carried out in a mixed-flow hydrothermal reactor as described by Dove and Crerar (1990) and Berger et al. (1994). One to ten grams of glass were tested with flow rates ranging from 1 to 9 ml min^{-1}. The size fraction of the particles was between 125 μm and 250 μm (Table 2). Under these conditions, the outflowing solution reached a steady-state composition after 3–10 h. After this time, solution aliquots were sampled and the glass dissolution rate was calculated at several time intervals based on the silica release for sphene and zirconolite glasses using Eq. (1) and from the nitrogen release for SiAlON glass using Eq. (2). Preliminary solution analysis (with the colorimetric method Aquamerck® 8024) showed that nitrogen is released from SiAlON glass as ammonium (NH_4^+).

$$r = \frac{vC_{Si}}{60\,000S} \quad (1)$$

$$r = \frac{vC_{NH_4}}{60\,000SX_{Si/N}}, \quad (2)$$

where r is the glass dissolution rate (mol Si m^{-2} s^{-1}), v the flow rate (ml min^{-1}), C_{Si} the Si concentration (mol l^{-1}) in the outflowing solution, C_{NH_4} the NH_4^+ concentration (mol l^{-1}) in the outflowing solution, S the specimen surface area (m^2) and $X_{Si/N}$ the Si/N molal ratio in the glass. The dissolution rates were also expressed in grams of glass per square meter per day. At the end of each experiment, the altered powder samples were recovered and prepared for solid characterization.

2.2.2. Closed-system experiments

For the static leaching experiments, powder specimens of 40–50 μm grain size fraction (Table 2) were placed in Teflon® containers with 5 ml of pure water to obtain a glass-surface-area-to-leaching-solution-volume (SA/V) ratio of 200 cm^{-1}. The test containers were then placed in flasks with a small quantity of water to minimize leakage by equalizing the pressures inside and outside the containers. The flasks were placed on a stirring device in a temperature-regulated chamber at 90 ± 0.1°C for periods of 1 week to 3 months. Seven to ten reaction time intervals were tested for each material. The altered grains were then rinsed, oven-dried at 90°C and prepared for solid characterization studies. The possible extent of colloids was assessed on a few samples ultrafiltered to 10 000 Da using Centricon® 10 filters (3 nm pore diameter) before dilution. The 'saturation' dissolution rates were determined by logarithmic regression from the normalized mass losses NL(i) calculated from Eq. (3):

$$\mathrm{NL}(i) = \frac{C_i \times 1000}{f_i \times \frac{SA}{V}}, \qquad (3)$$

where i, C_i, f_i and SA/V are the corrosion tracer element, its concentration (g l^{-1}) in the leachates, the mass fraction of element i in the glass, and the glass-surface-area-to-leaching-solution-volume ratio (m^{-1}), respectively. NL(i) values are calculated at each sampling time, and expressed in g m^{-2}.

2.3. Analytical methods

2.3.1. Solution analysis

The leachates were analyzed for aqueous silica using the molybdate colorimetry method (Strickland and Parksons, 1972), for NH_4^+ by colorimetry of complexation with sodium salicylate and chlorine in an alkaline medium, for Ca and Al by emission/absorption spectrometry (Perkin-Elmer Zeemann 5000), for Ti, Zr and Nd by inductively coupled plasma mass spectrometry (ICP-MS; Perkin-Elmer Elan 5000). The leachate pH was measured at 25°C, while minimizing atmospheric CO_2 exchanges.

2.3.2. Solid analysis

The initial and altered samples were examined by X-ray diffraction (XRD; Phillips PW 1130 apparatus and X-ray database reference file ICDD). Raw altered powder specimens and ultrathin cross-sections were observed with a scanning electron microscope (SEM; Jeol 6400) with EDS/WDS, and with a transmission electron microscope (TEM; Phillips 120 kV) with an EDS. The chemical compositions of thin sections of altered powders were submitted to microprobe analysis (SX50 Camebax) and the chemical composition of the subsurface was determined by X-ray photoelectron spectroscopy (XPS; Escalab NK2) on raw altered grains. For the XPS analyses, we verified that the measured peak surface area ratios of Si, Al and Nd were proportional to their concentration ratios in the pristine solid for various glass compositions.

3. Results

The leachate chemical analysis results are indicated in Tables 3–5.

3.1. Open-system experiments

The glass dissolution stoichiometry is shown in Fig. 1.

3.1.1. Sphene glass

At the three test temperatures, the release of the network former into solution was stoichiometric with respect to Si in the glass (Fig. 1). Conversely, Nd and Ti were only slightly solubilized and were probably incorporated in secondary phases. Calcium was partially retained in the secondary phases in the most highly concentrated leachates. Examples of calculated rates and measured pH values are shown in

Table 3
Experimental data for sphene and zirconolite glass dissolution in renewed deionized water at 90, 150 and 200°C (constant stirring speed at 450 rpm for all tests)

Time (h)	Flow rate (ml min^{-1})	Surface area (cm^2)	pH (25°C)	Si (ppm)	Al (ppm)	Ca (ppm)	Ti (ppb)	Zr (ppb)	Nd (ppb)	Rate (mol Si m^{-2} s^{-1})	Rate (g m^{-2} d^{-1})
Sphene glass 125–250 μm, T = 90°C											
3	8.94	903	6.10	0.47	0.04	0.16	0.50		0.90	2.76E-08	0.35
20	1.04	903	6.70	1.58	0.14	0.97	4.50		3.90	1.08E-08	0.14
52	1.04	903	7.74	3.20	0.98	1.77	26.70		25.60	2.19E-08	0.28
92	1.08	903	8.01	3.29	0.97	1.77	21.40		20.80	2.33E-08	0.30
164	1.05	903	7.24	3.32	1.22	1.72	14.30		13.90	2.29E-08	0.29
260	1.08	903	7.42	3.39	1.32	1.72	6.90		6.30	2.41E-08	0.31
Sphene glass 125–250 μm, T = 150°C											
3	8.91	903	9.10	7.47						4.37E-07	5.58
18	2.57	903	9.50	10.45						1.76E-07	2.25
27	2.57	903	8.13	10.91						1.84E-07	2.35
Sphene glass 125–250 μm, T = 200°C											
3	8.81	291	9.03	9.12	3.11	3.00			0.50	1.64E-06	20.89
18	2.47	271	9.58	12.25	4.00	2.81			0.10	6.62E-07	8.45
43	2.49	241	9.58	9.76	3.89	2.92			0.40	5.98E-07	7.63
66	2.51	216	9.38	7.80	3.44	3.05			0.10	5.38E-07	6.86
91	2.48	197	9.30	5.12	2.44	2.50			0.40	3.82E-07	4.88
114	2.56	185	9.15	3.00	1.10	1.91	2.00		2.00	2.46E-07	3.14
139	2.57	178	8.68	1.60	0.40	1.17	0.90		0.60	1.37E-07	1.75
161	2.53	174	8.29	0.93	0.28	0.73	1.40		1.00	8.02E-08	1.02
Zirconolite glass 125–250 μm, T = 90°C											
23.5	0.99	740	8.15	2.06	0.76	1.55	6.55	3.98	66.40	1.64E-08	0.21
47	0.96	740	7.92	2.20	0.76	1.73	17.70	10.50	58.50	1.69E-08	0.22
71	0.93	740	7.97	2.25	0.76	1.74	14.50	9.20	32.10	1.68E-08	0.21
144	0.93	740	8.16	2.20	0.76	1.68	7.53	5.25	13.50	1.64E-08	0.21
Zirconolite glass 125–250 μm, T = 150°C											
10.7	2.41	740	8.87	7.75	2.56	6.30		0.27	0.35	1.50E-07	1.91
22	2.52	740	9.12	7.75	2.46	6.46		0.12	0.26	1.57E-07	1.99
Zirconolite glass 125–250 μm, T = 200°C											
3.2	8.68	740	9.37	9.00	3.22	7.20		0.05	0.18	6.26E-07	7.98
7.5	8.69	740	9.30	9.50	3.12	7.53		0.04	0.30	6.62E-07	8.43
9.8	8.70	740	9.27	8.25	3.12	7.53		0.05	0.28	5.75E-07	7.33
6	4.15	493	9.68	9.75	3.60	6.50				4.87E-07	6.21
19.5	4.18	468	9.24	10.00	3.59	7.55				5.30E-07	6.75
43.5	4.60	444	9.63	9.62	3.50	7.51				5.91E-07	7.53
47.5	8.95	443	9.63	7.68	2.94					9.21E-07	11.73
66.5	4.21	404	9.59	7.89	3.20	7.13				4.88E-07	6.21
90.5	1.41	375	9.75	9.47	3.52	9.71				2.11E-07	2.69
16	2.36	110	9.39	7.45	3.18	5.75				9.50E-07	12.10
19	9.00	107	9.40	4.91	2.11	3.65				2.45E-06	31.21
23.5	6.08	103	9.20	5.31	2.33	4.09				1.86E-06	23.69
28.5	4.25	98	9.27	5.53	2.45	4.46				1.42E-06	18.13

Table 4
Experimental data for SiAlON glass dissolution in renewed medium at 90, 150 and 200°C

Time (h)	Flow rate (ml min^{-1})	Surface area (cm^2)	pH (25°C)	Si (ppm)	Nd (ppb)	Al (ppb)	N (ppb)	Rate (mole Si m^{-2} s^{-1})	Rate (g m^{-2} d^{-1})	Stirring speed (rpm)
Pure water, T = 200°C										
3	8.27	277	7.5	0.21	52	45	46	7.47E-08	1.19	450
5.7	8.32	277	7.4	0.2	97	92	42	6.86E-08	1.09	
23	2.58	277	6.72	0.68	199	69	100	5.07E-08	0.81	
72.2	2.59	277	6.4	0.65	81	46	90	4.58E-08	0.73	
3.7	8.96	9400	6.9	1.32	47	53	165	8.56E-09	0.14	750
6.8	8.92	9400	6.8	0.96	54	46	121	6.25E-09	0.10	
5	5	1880	6.15	0.59	70	23	100	1.45E-08	0.23	450
10.3	5.01	1880	5.39	0.95	301	21	130	1.88E-08	0.30	750
15.6	5.05	1880	5.8	0.7	63	20	100	1.46E-08	0.23	450
24.4	2.52	1880	6.45	0.86	45	21	150	1.09E-08	0.17	
32.8	2.57	1880	6.45	0.84	43	18	140	1.04E-08	0.17	
55.2	1.05	1880	6.07	1.58	44	13	164	4.98E-09	0.08	
76.1	1.08	1880	6.18	1.5	47	12	192	6.00E-09	0.10	
15.5	2.55	277	6.4	0.84	116	18	52	2.60E-08	0.42	450
39.1	2.58	277	5.79	0.98	105		95	4.81E-08	0.77	750
48.6	2.58	277	5.57	0.91	95	20	104	5.27E-08	0.84	750
67.7	2.61	277	5.7	1.02	65	33				1050
24	0.943	9400	7.18	2.87	5.1	86.8	443	2.42E-09	0.04	900
41	2.394	9400	7.53	1.27	73.7	20.1	190	2.63E-09	0.04	
44.5	8.51	9400	7.45	0.775	90.5	26.2	139	6.85E-09	0.11	
47.5	8.46	9400	7.7	0.875	94.7		190	9.30E-09	0.15	1500
50.5	8.54	9400	6.36	0.775	90.7		124	6.13E-09	0.10	
65.5	2.34	9400	6.67	1.4	39.9	22.5	185	2.51E-09	0.04	450
3	8.91	277	8.05	1.12	303	25	144	2.52E-07	4.02	1500
7	4.83	277	7.52	1.32	979	30.5	177	1.68E-07	2.68	
19	1.93	277	7.38	1.5	1219	26	195	7.39E-08	1.18	
44	0.936	277	7.22	1.77	597	17.7	225	4.14E-08	0.66	
47.2	8.7	277	7.65	0.8	116	26.7	106	1.81E-07	2.89	
Glass without nitrogen, pure water, T = 200°C										
3.5	8.98	277	6.19	0.573	534	21.9	4.08	8.76E-08	1.35	1500
17	1.86	277	5.7	1.459	335	16.3	12.81	5.70E-08	0.88	
Decarbonated pure water, T = 200°C										
3.25	8.78	277	6.46	0.695	97.1	32.2	120	2.07E-07	3.30	1500
15	1.72	277	6.05	1.74	28.5	14.2	196	6.62E-08	1.06	
10^{-2} M Na_2SO_4, T = 200°C										
3	8.92	277	8.65	8.26	9.65	3192	960	1.68E-06	26.80	1500
14	1.78	277	8.29	10.21	4.3	3794	1480	5.17E-07	8.25	
19.5	3.93	277	8.74	8.04	5.72	3226	1040	8.03E-07	12.79	
10^{-1} M Na_2SO_4, T = 200°C										
3	9.04	83.1	8.55	6.35	1214	2600	690	4.08E-06	65.07	1050
17	2.44	83.1	8.54	7.1	380	2690	780	1.25E-06	19.86	
Pure water, T = 90°C										
18.1	1.15	9400	7.2	1.26	1036	759	500	3.33E-09	0.05	750
39.8	1.03	9400	7.27	1.27	2	396	346	2.06E-09	0.03	
46	1.017	9400	7.02	1.25	3	386	283	1.67E-09	0.03	450
96	1.004	9400	7.63	1.32	22.3	218	220	1.28E-09	0.02	

Table 4 (continued)

Time (h)	Flow rate (ml min^{-1})	Surface area (cm^2)	pH (25°C)	Si (ppm)	Nd (ppb)	Al (ppb)	N (ppb)	Rate (mole Si m^{-2} s^{-1})	Rate (g m^{-2} d^{-1})	Stirring speed (rpm)
Pure water, T = 90°C										
142	1	9400	7.95	1.3	45.2	248	149	8.62E-10	0.01	
173	0.971	9400	7.24	2.18	36.1	234	180	1.01E-09	0.02	900
10^{-2} M Na_2SO_4, T = 90°C										
17	1.94	831	5.95	1.08	57.2	320.7	116	1.47E-08	0.23	1500
10^{-1} M Na_2SO_4, T = 90°C										
8	2.16	831	7.03	1.58	1293	640	240	3.39E-08	0.54	1050
Pure water, T = 150°C										
5.2	7.6	9400	7.08	1.7	20	183	160	7.04E-09	0.11	750
21.1	2.51	9400	7.01	1.85	9	158	230	3.34E-09	0.05	
10^{-2} M Na_2SO_4, T = 150°C										
3.7	9.07	831	7.56	3.71	4529	1440	380	2.26E-07	3.60	1500
10^{-1} M Na_2SO_4, T = 150°C										
11	8.62	831	7.28	4.18	727	1590	500	2.82E-07	4.50	1050

Fig. 2 and reported in Table 3. At 200°C, dissolution resulted in a 55% specimen mass loss; the reduction in the reactive surface area due to dissolution of the grains was calculated by assuming a geometric reduction of spherical grains. At this temperature, the dissolution rate diminished over time (Figs. 2 and 3), while the pH (measured at 25°C) varied between 8.3 and 9.6. It is important to note that the 'initial' rates were measured after 3 h of leaching and could well be lower than the true initial rates, which cannot be measured experimentally. The drop in the dissolution rate, at 200°C, could be attributed to a protective effect of secondary phases, as observed with basalt glass by Berger et al. (1994). At 90°C, with the exception of the second sampling interval, no drop in the dissolution rate is observed with the progress of the reaction, during 300 h (Table 3).

3.1.2. Zirconolite glass

The leachate composition and pH were similar to those obtained with sphene glass (Table 3). The pH fluctuated around 8 and 9, and the release of Al and Ca was stoichiometric with respect to Si (Fig. 1). The release of Ti, Zr and Nd was highly incongruent, with very low concentrations in solution (Fig. 1). However, no drop in the dissolution rate was observed over time under constant experimental conditions, even after 90 h at 200°C (Fig. 2), but the dissolution rate was dependent on the solution flow rate and the reactive surface area. This reversible dependence on the experimental conditions is illustrated in Fig. 3, which shows the dissolution rate measured at 200°C vs. a flow rate/surface area term. The observed dependence—and especially its reversibility—suggests rate control by chemical affinity control of the reaction, since the most concentrated leachates and the lowest rates corresponded to the lowest values of the flow rate/surface area ratio. It must be noted, however, that the silica concentrations in all the leachates were well below the silica concentration at saturation with respect to amorphous silica, as reported in the literature (>200 ppm), and varied only slightly (from 4 to 10 ppm).

3.1.3. SiAlON glass

SiAlON glass differs from the two discussed above by its high Nd concentration (53.8 wt.% Nd_2O_3) and by the absence of alkaline earth elements. In addition to the experiments in deionized water, other tests were conducted in decarbonated pure water (after degassing at 10^{-2} Torr) and with Na_2SO_4 solutions complexing the rare earth elements (Ménard, 1995; Ménard et al., 1998).

In deionized water, with or without prior decarbonation, SiAlON glass dissolution is highly incongruent for Al and Nd, which is less solubilized than

Table 5
Experimental data for closed system dissolution of zirconolite, sphene and SiAlON glasses at 90°C ($SA/V = 200\ cm^{-1}$) in initially pure water

Time (days)	pH (25°C)	Si (ppm)	Al	Ca	N	Nd	Ti	Zr	Filtration of the leachates prior to analysis
Zirconolite glass									
13	8.26	44.55	2.34	6.25		2.180	0.330	0.250	0.45 μm filters
26	7.66	49.75	0.48			0.005	< 0.001	0.001	UF[a]
40	8.20	48.25	2.40	12.60		1.060	1.650	1.200	0.45 μm filters
48	8.11	46.25	1.30	7.84		0.014	< 0.001	0.010	UF
68	8.07	54.17	2.00	28.20		1.310	2.040	1.530	0.45 μm filters
81	8.29	54.55	0.24			0.007	< 0.001	0.004	UF
94	7.47	40.75	1.45	26.80		0.816	1.270	0.965	0.45 μm filters
Sphene glass									
6	7.57	16.74	1.18	9.20		< 0.001	< 0.001		
15	7.24	32.73	2.07	21.14		2.411	2.089		0.45 μm filters
21	7.78	20.60	1.21	19.55		0.017	0.006		UF
27	8.99	24.18	2.47	16.39		1.898	1.688		0.45 μm filters
33	8.26	36.30	1.41	26.80		1.181	1.022		0.45 μm filters
42	7.36	35.80	0.88	26.80		0.008	< 0.001		UF
59	8.15	34.40	2.69	24.59		2.332	2.083		0.45 μm filters
76	7.65	30.00	0.55	24.69		0.037	0.019		UF
84	7.32	46.30	1.04	35.67		3.212	2.676		0.45 μm filters
105	7.78	37.27	1.78	27.82		1.995	1.710		0.45 μm filters
SiAlON glass									
6	9.20	4.65	11.19		23.09				0.45 μm filters
15	7.28	38.18	3.92		15.44	49.106			0.45 μm filters
21	8.88	11.40	3.40		22.06	0.030			UF
27	9.63	20.66	14.35		24.40	40.362			0.45 μm filters
33	8.25	35.30	10.85		20.15	71.903			0.45 μm filters
42	7.64	40.00	0.56		23.53	0.005			UF
59	8.09	52.10	16.85		27.20	44.399			0.45 μm filters
76	8.33	40.09	8.54		28.23	0.013			UF
84	7.30	47.22	8.54		24.70	171.26			0.45 μm filters
105	7.95	57.27	33.16		28.97	125.72			0.45 μm filters

[a]UF: Ultrafiltration of the leachates with Centricon® 10 filters (3 nm pore diameter).

Si, all with respect to N (Fig. 1). The nearly neutral leachate pH could account for the incongruence of aluminum by precipitation of aluminum hydroxide, since the measured Al concentrations are very close to the boehmite solubility in neutral solution at 200°C (near 10^{-6} mole/kg at $pH_{200°C} = 5.5$; Bourcier et al., 1993; Castet et al., 1993). Dissolution was roughly stoichiometric in general for Si. The measured rates in pure water were very low in comparison with the other glasses, and poorly reproducible. Numerous tests were carried out at 200°C to obtain a better understanding of this glass. The lowest values measured at 200°C were on the order of 0.05 g m^{-2} d^{-1}, or about three orders of magnitude lower than for the sphene, zirconolite, tholeitic basalt glass and R7T7 glass samples. In addition, the 'initial' dissolution rates differed considerably according to the experimental conditions (stirring speed, grain size, reactive surface area) and even according to the leaching solution composition. Fig. 4 shows that the SiAlON glass dissolution rate at 200°C in deionized water was linearly dependent on the parameters quantifying the leaching medium undersaturation (flow rate/reactive surface area) and on the grain surface concentration gradients disturbed by stirring (stirring speed). A deposit was observed on the

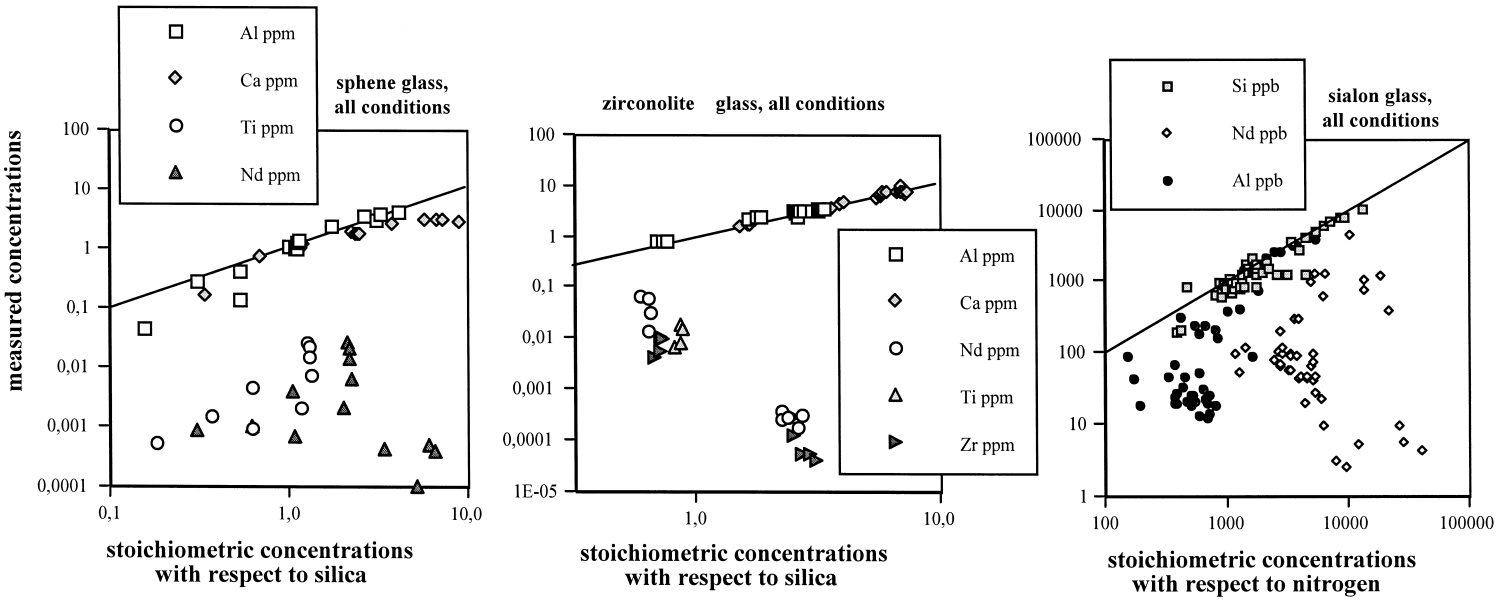

Fig. 1. Measured concentrations (y-axis) of glass components in solution from mixed-flow reactor at 200°C, as a function of the stoechiometric concentrations (x-axis) with respect to Si (for sphene and zirconolite glasses) or N (for SiAlON glass). The stoichiometric concentrations reported on the x-axis were calculated as: ($C_{(j)\text{leachate}} \times$percentage i_{glass})/percentage j_{glass}, where $C_{(j)\text{leachate}}$ is the concentration of Si (sphene and zirconolite glasses) or N (SiAlON glass) in the leachate in parts per million, (percentage i_{glass}) is the percentage weight of the element i in the sound glass and percentage j_{glass} is the percentage weight of Si or N in the sound glass. The straight lines represent the stoichiometric release of the components with respect to Si (a,b) or N (c).

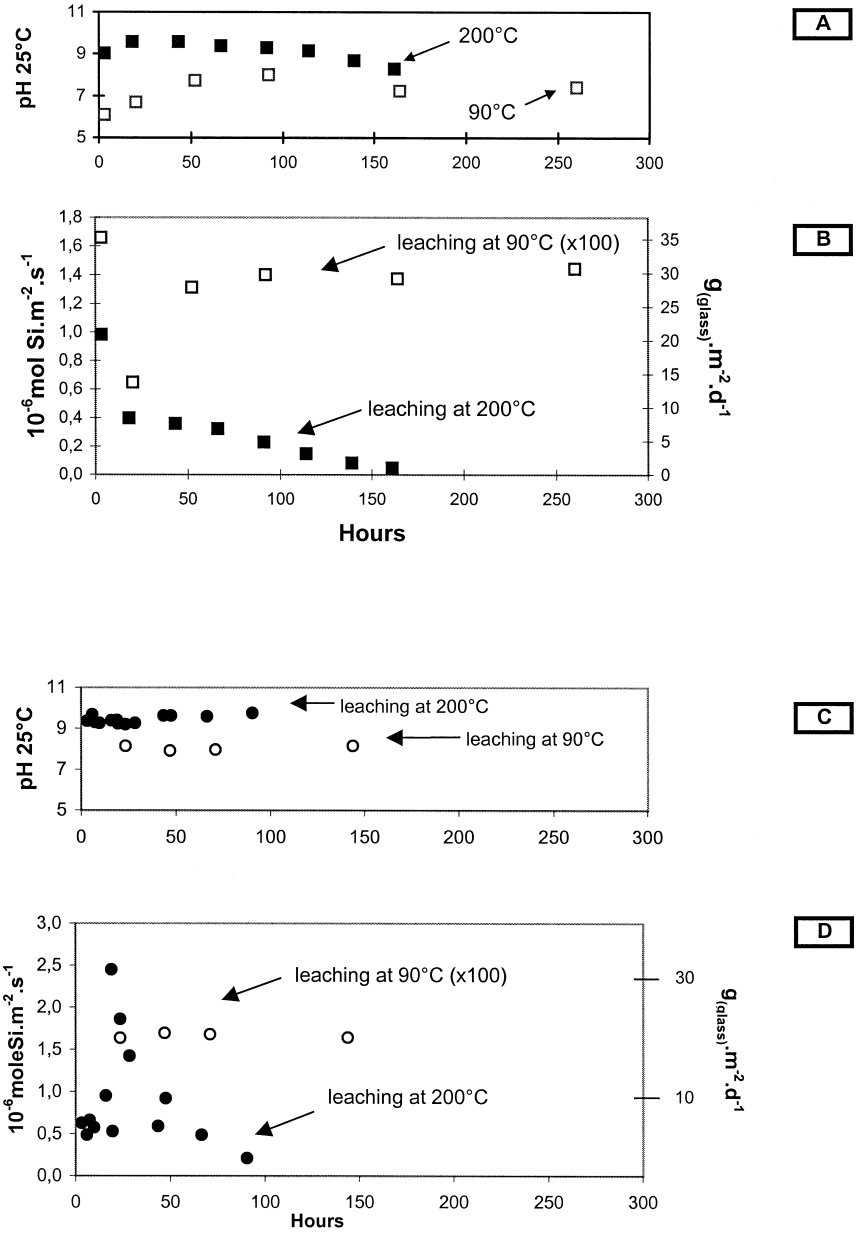

Fig. 2. Sphene glass dissolution rate at 90 and 200°C (graphs A and B), and zirconolite glass dissolution at 90°C and 200°C (graphs C and D), in mixed-flow reactor.

reactor walls at the end of these experiments, and was identified by X-ray diffraction as a layer of hydrated neodymium carbonate (X-ray diffraction reference file, ICDD 27-1296). The rate obtained in decarbonated water was the same as observed under the same conditions with deionized water at equilibrium with the atmosphere. Two additional experiments at 200°C (flow rates equal to 8.98 and 1.86 ml mn^{-1}) with an equivalent glass containing no nitrogen yielded the same kinetic results (Table 4). These

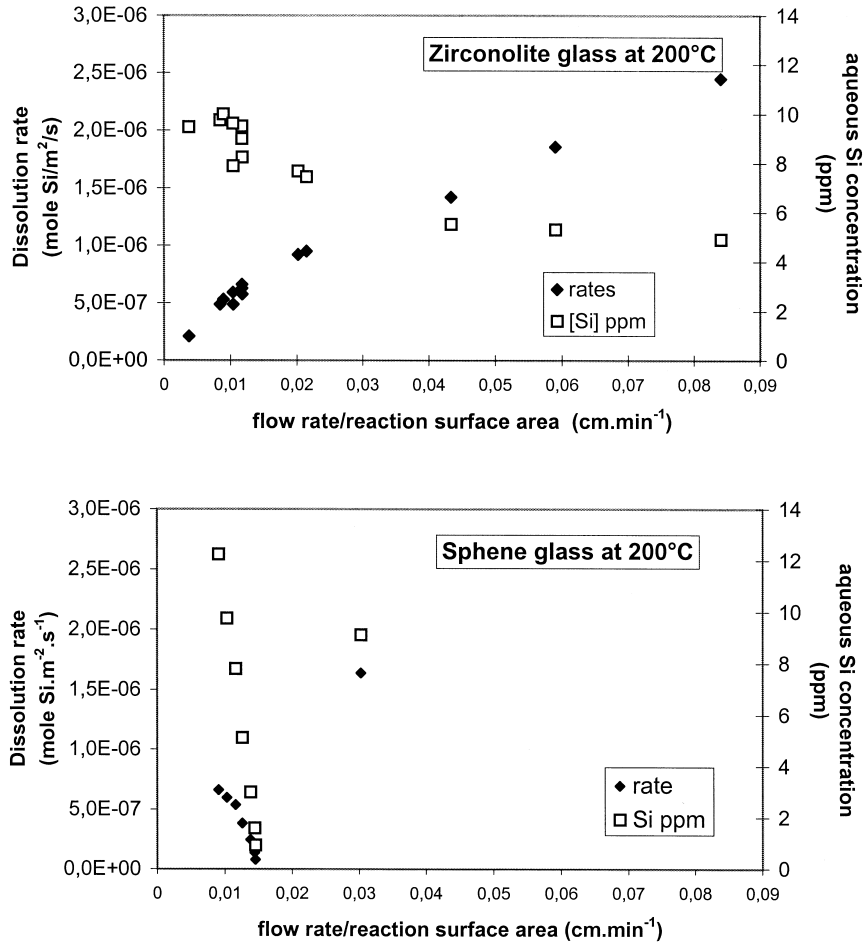

Fig. 3. Influence of experimental conditions on zirconolite glass and sphene glass dissolution rates in initially pure water at 200°C.

complementary results demonstrate that nitrogen does not improve the chemical durability of an oxide-based glass.

Unlike the pure water experiments, 0.01 M and 0.1 M sodium sulfate solutions resulted in higher and more reproducible alteration rates near those of the other aluminosilicate glasses tested. Moreover, the resulting leachates were depleted only in Nd compared with the stoichiometry of the pristine glass (Fig. 1 and Table 4); this depletion was due to the observed precipitation of a mixture of neodymium oxide, neodymium oxysulfate and hydrated neodymium carbonate (X-ray diffraction patterns ref. ICDD 23-1261, 28-671, 6-408, 24-775) and an unidentified phase (6.88, 6.30, 5.25, 5.01, 4.70, 4.35, 4.10, 3.14, 2.74 Å) that could be a double Nd–Na sulfate. This precipitation may be correlated with the diminution of the glass dissolution rate, by 50% after 15 h of leaching under these conditions. However, it is important to note that the alteration solution flow rate was diminished during the experiment with a 10^{-2} M Na_2SO_4 enriched solution, from 8.92 to 1.78 ml min^{-1}, and then was increased again to 3.93 (Table 4). The variation of the dissolution rate was rather related to the flow rate variation (and not to a protective effect of the alteration layer), as in the case of the zirconolite glass.

The stoichiometry of aluminum release with respect to Si and N (Fig. 1, values between 1000 and 10 000 on the abscise axis) was probably due to the

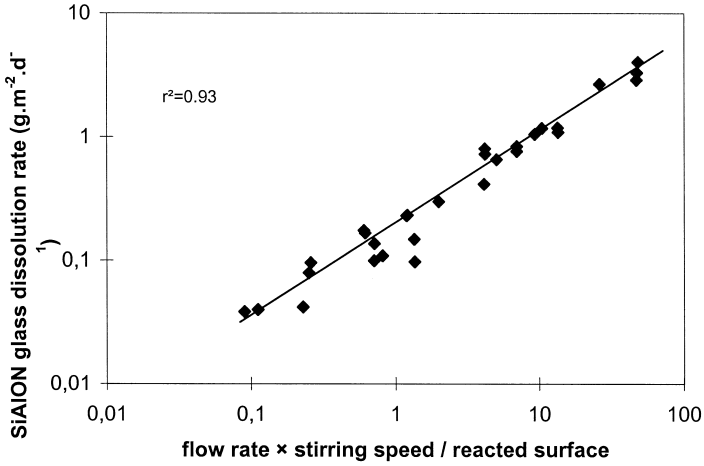

Fig. 4. Dependence of SiAlON glass dissolution rate in pure water at 200°C on the experimental conditions.

higher pH obtained in these experiments (increased solubility of aluminum hydroxides), which in turn can be attributed to greater hydrolysis of the glass.

3.1.4. Characterization of altered glass powders

Only the sphene, zirconolite and SiAlON grains altered at 200°C were investigated by scanning electron microscopy (Fig. 5A–C), microprobe analysis and X-ray photoelectron spectroscopy. SEM observation revealed a newly formed layer on the surface of the sphene glass (Fig. 5B); the backscattered electron image indicated that this layer was enriched with Nd. The layer appeared to be much more limited on the zirconolite glass, where only denser zones were visible at $\times 10\,000$ magnification (Fig. 5A). However, electron microprobe examination of polished cross-sections revealed the existence of highly developed alteration zones covering up to a third of the zirconolite grains (Leturcq, 1998). Chemical variations at the surface of the altered grains, for the sphene and zirconolite glasses, are shown in Table 6 in the form of elemental ratios normalized with respect to the pristine glass; these zones can be seen to be enriched with heavy elements (Zr and Nd). The alteration layer observed by SEM on the SiAlON glass was much more massive, reaching a thickness of several micrometers (Fig. 5C). Needle-shaped crystals were observed (Fig. 5C) in this alteration layer; ESCA analysis showed surface enrichment in Nd (Table 7), relative to Si. The presence of a hydrated neodymium carbonate was also determined by XRD (ICDD: 27-1296).

3.2. Closed-system experiments (at 90°C)

In closed-system experiments, the leachates reached more or less steady-state conditions for all three glasses, as shown in Fig. 6. The silica concentrations at the end of each experiment conducted at 90°C ranged from 40 to 60 ppm, and the pH at 25°C from 7.5 to 9 (Table 5). The concentrations of the metallic elements (Al, Ti, Zr, Nd) were more variable, and the low values (a few parts per billion) measured after ultrafiltration (on filters with 3 nm pore diameter) suggest that they were present at least partially in colloid or particle form.

With SiAlON glass, Si, Al (before ultrafiltration) and N dissolved congruently after an initial preferential release of nitrogen, resulting in a 16-nm nitrogen-depleted layer. The thickness was estimated by

Fig. 5. SEM observations of glasses altered in renewed pure water at 200°C. (A) Zirconolite glass altered for 90 h. (B) Sphene glass altered for 161 h. (C) SiAlON glass altered for 76 h.

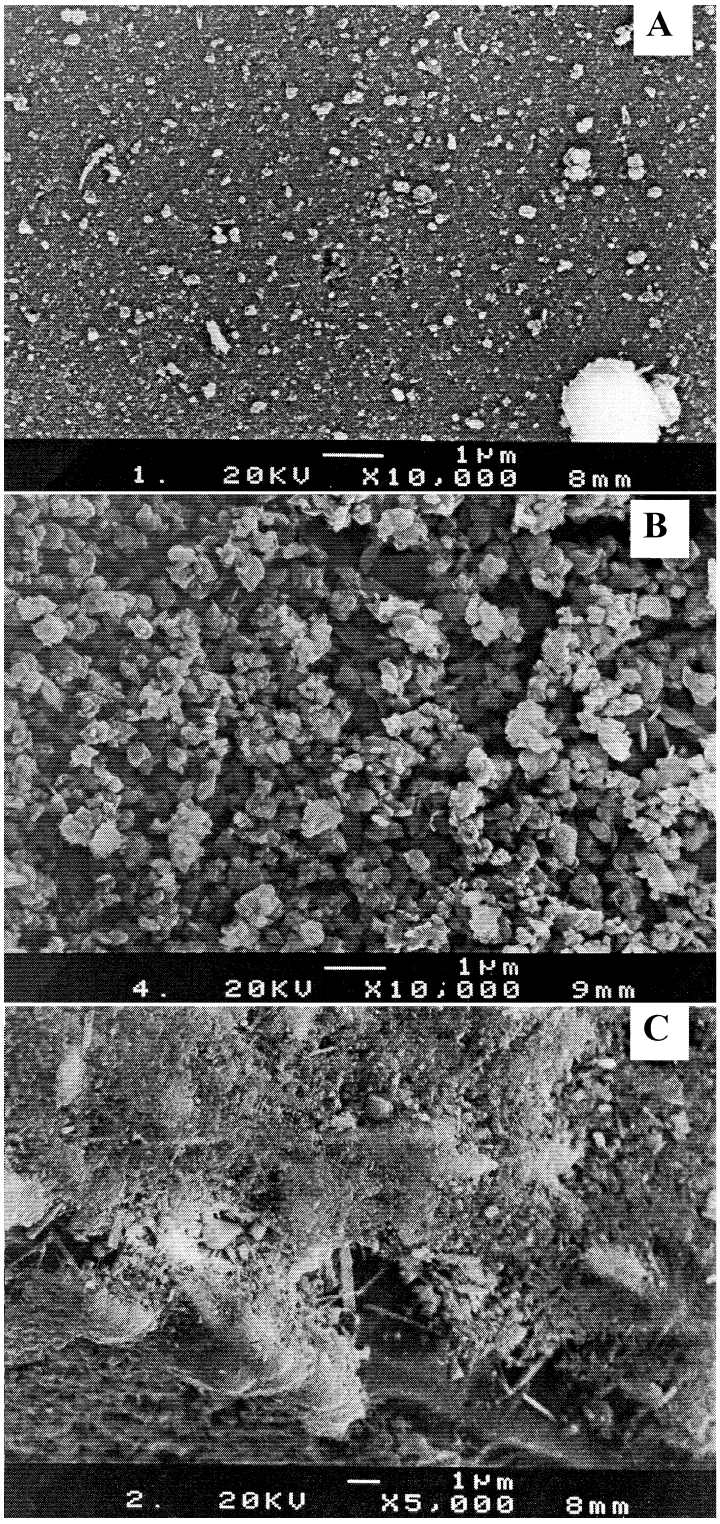
A
1μm
1. 20KV X10,000 8mm
B
1μm
4. 20KV X10,000 9mm
C
1μm
2. 20KV X5,000 8mm

Table 6
Evolution of chemical composition between fresh glass (zirconolite and sphene glasses) and alteration film on grains altered in open system at 200°C

Glass	$(Ca/Si)/(Ca/Si)_0$	$(Al/Si)/(Al/Si)_0$	$(Ti/Si)/(Ti/Si)_0$	$(Nd/Si)/(Nd/Si)_0$	$(Zr/Si)/(Zr/Si)_0$
Zirconolite	1.32	0.69	5.12	4.90	5.08
σ^2	0.11	0.02	0.02	0.04	0.07
Sphene	0.91	0.78	4.44	4.20	–
σ^2	0.09	0.09	0.33	0.26	–

Me/Si ratios determined by electron microprobe (six analyses per glass and per element).

dividing the normalized mass loss of N (see Eq. (3)) by the specific gravity (4 g cm^{-3}) of the SiAlON glass (Leturcq et al., 1997).

Neodymium was found in solution partially in particle or polymerized form, as was a fraction of the aluminum, because lower concentrations were analyzed after ultrafiltration, with respect to the concentrations determined after filtration through 0.45 μm filters (Leturcq, 1998; Leturcq et al., 1997). For the sphene glass, Ca dissolution appeared to be congruent with respect to Si, while Al, Ti and Nd were only slightly solubilized. The dissolution of zirconolite glass was totally incongruent for all the elements (including Ca) with respect to Si.

The dissolution rate of SiAlON glass can easily be determined under saturation conditions by using nitrogen as a corrosion tracer.

Fig. 7 shows the normalized mass losses (Eq. (3)) on a logarithmic time scale. The alteration rate thus diminishes with the reaction progress according to a relation of the type $r = a(1/t)$, where a is the constant preceding the logarithm and t is the time. The high initial normalized mass loss value for nitrogen characterized the preferential release of nitrogen during the first instants of dissolution. The saturation rate is more difficult to determine for sphene and zirconolite glass due to the absence of a suitable dissolution tracer. The rates measured from the silica concentrations in the leachate are in fact minimum estimates, since a fraction of the silica may have been trapped in the alteration phases. Table 8 indicates the alteration rate for SiAlON glass (based on N release) after 100 days of leaching, together with the minimum estimates for sphene and zirconolite glass (based on Si release). These rates are four orders of magnitude lower than the initial dissolution rate.

SEM and TEM examination of the altered samples did not reveal conclusive evidence of chemical or morphological transformations of the grain surface. However, a zone of reduced electron contrast some 50 nm thick was observed at the SiAlON glass/solution interface by TEM, and could constitute an altered zone (Fig. 8). Chemical changes were recorded on altered SiAlON glass by XPS (Table 7): the proportions of Al increase with respect to Si, while the opposite is true for Nd. This suggests the existence of a very thin layer enriched with Al and Si, a hypothesis corroborated by specific area measurements of the SiAlON glass: the surface area increased from 0.094 before the experiments to 0.278 m^2 g^{-1} after the experiments. This aluminosilicate

Table 7
XPS analysis of SiAlON glass altered in closed system at 90°C and in open system at 200°C

	Peak area ratio					
	Fresh glass	Closed system (90°C)				Open system (200°C)
		27 days	42 days	75 days	105 days	
Al_{2p}/Si_{2p}	0.27	0.66	0.52	0.42	0.45	0.35
$Nd_{3d5/2}/Si_{2p}$	2.79	0.66	0.28	0.48	0.58	8.73

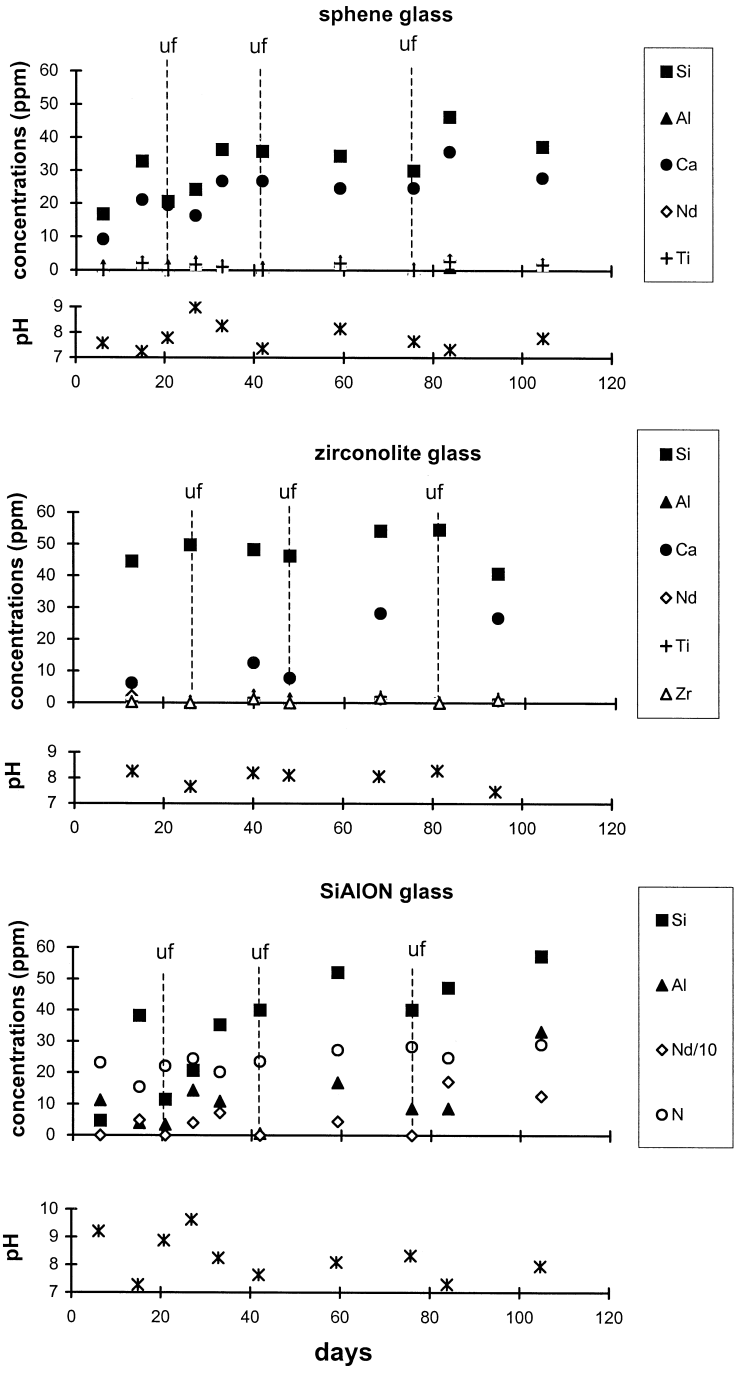

Fig. 6. Change of solution chemistry during closed-system experiments (90°C, pure water, $SA/V = 200\ cm^{-1}$). uf = Ultrafiltered.

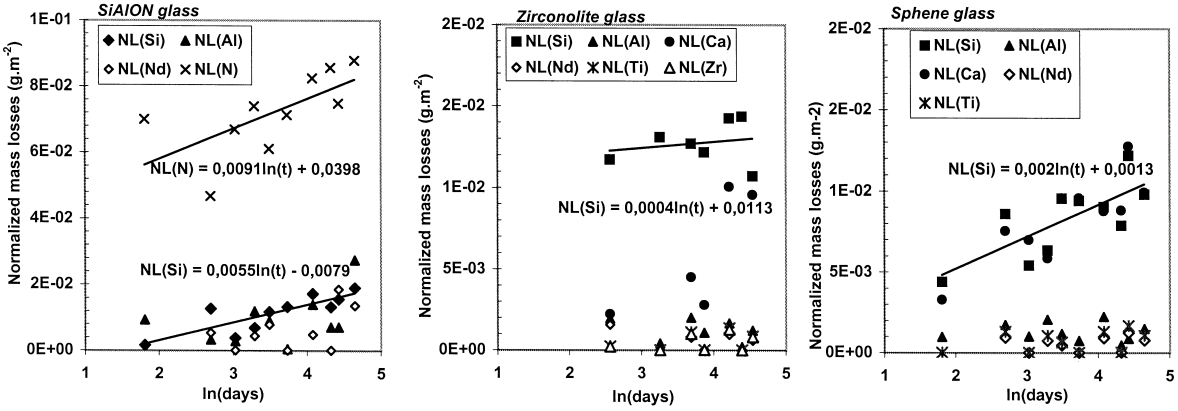

Fig. 7. Evolution of normalized mass losses during static leach tests at 90°C and $SA/V = 200\ cm^{-1}$. Fitted logarithmic functions were used to determine the dissolution rates.

skin would likely be formed by the high aqueous silica and aluminum concentrations.

4. Discussion

4.1. Initial dissolution rates at low reaction progress

4.1.1. SiAlON glass

The dependence of the 'initial' dissolution rate of SiAlON glass at 200°C in deionized water on the experimental conditions, such as the flowing rate and the stirring speed) (Fig. 4) suggests that the kinetics are controlled by diffusion of aqueous species near the reaction interface.

In the light of previous work on other silicate glasses (R7T7, tholeites) showing a chemical reaction affinity effect for much higher Si (>100 ppm) concentrations (Grambow, 1985; Berger et al., 1994), the Si concentrations in the leachates (<2 ppm) cannot account for the low measured rates unless a very high concentration gradient is assumed near the reactive surface. The observed precipitation of neodymium carbonate-enriched layer cannot account for a hypothetical Si concentration gradient that would explain the low measured rates, since the

Table 8
Dissolution rates (g_{glass} m^{-2} d^{-1}) for the SiAlON, sphene and zirconolite glasses after 100 days of leaching at 90°C in closed system at $SA/V = 200\ cm^{-1}$

SiAlON	Sphene	Zirconolite
1.05×10^{-4} [a]	1.8×10^{-5} [b]	1.3×10^{-5} [b]

[a] Dissolution rate based on N release.
[b] Minimum estimate based on Si release.

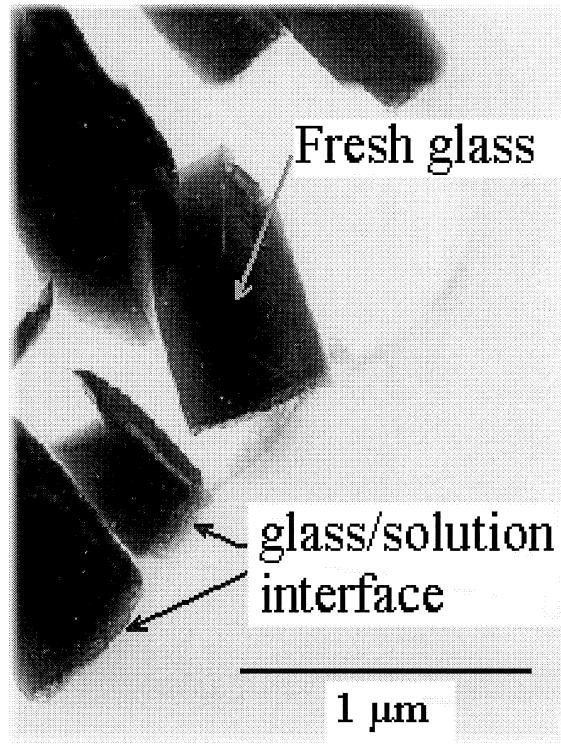

Fig. 8. TEM observations of SiAlON glass samples altered in pure water at 90°C for 105 days in closed medium. The thin altered zone is located on the left parts of the glass shards (glass/solution interface).

same low alteration rates were noted in the absence of carbonates. If this hypothetical strong Si concentration gradient is excluded, the only reaction capable of controlling the dissolution kinetics of this SiAlON glass in pure water appears to be hydrolysis of the Nd–O bonds (the additional experiment with a nitrogen-free glass showed that nitrogen has no effect on the chemical durability of the glass). A 'passivation' effect resulting from the development of a slightly reactive Nd-enriched surface layer could account for the low measured rates. Indeed, if a suitable complexing agent (Na_2SO_4) is used to prevent the formation of a Nd-enriched layer, typical (higher) dissolution rates of aluminosilicate glasses are again obtained for the SiAlON, i.e., 26.8 to 65 g m^{-2} d^{-1} at 200°C (Table 4). These last experiments highlight the passivating role of neodymium, when retained in the alteration layer, in a glass containing 53.8 wt.% Nd_2O_3 oxide. We therefore decided to consider the rates obtained with the sodium sulfate solution as characteristic of the initial dissolution phase of SiAlON glass; passivation by neodymium was considered as a subsequent alteration phase even though it occurs very quickly.

4.1.2. Initial dissolution rates at very low reaction progress

The initial dissolution rates of the three glass compositions tested between 90 and 200°C are indicated in Fig. 9 together with those of basaltic and R7T7 glasses. The data for the latter were compiled from published work by Crovisier et al. (1985, 1987), Berger et al. (1987, 1988, 1994), Guy (1989), Guy and Schott (1989), Caurel (1990), Advocat (1991) and Delage and Dussossoy (1991). Under experimental conditions where protective effects of the surface altered layers may be discarded (low reaction progress, high stirring rates, complexation by sulfate ions), the initial rates measured for sphene, zirconolite and SiAlON glass were very close and slightly lower than those of basalt glasses and R7T7 glass. The slight difference may be attributable to the fact that the reactive surface areas were not determined in the same manner. The dissolution rates of the basalt and R7T7 glasses are based on the geometric (macroscopic) surface area, while in the present study, we use the BET (microscopic) surface areas; a three- to four-fold difference between the macroscopic and microscopic surface area accounts for the observed

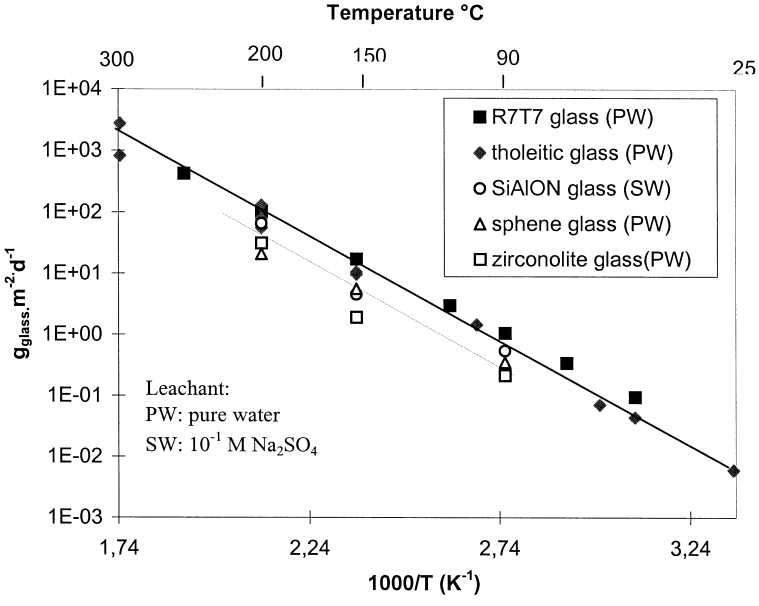

Fig. 9. Arrhenius plot showing initial dissolution rates for the three test glasses; comparison with published data on tholeitic basalt from Crovisier et al. (1985), Berger et al. (1987, 1988, 1994), Guy (1989), Guy and Schott (1989), Caurel (1990), and on R7T7 glasses from Advocat (1991) and Delage and Dussossoy (1991).

differences between the two sets of data. We therefore consider that the initial dissolution rates for all these glasses are the same. This result was predictable according to Berger (1995) and Guy and Schott (1989), since all these glasses are composed of the same network forming oxides (SiO_2 and Al_2O_3) in similar proportions. The initial dissolution rates and activation energies are indicated in Table 9. An uncertainty of 5 kJ mol^{-1} is assigned by assuming a systematic 20% error margin on the rate determinations, considering the number of factors involved (surface area measurement, sample weighing, pump flow rate, dilution errors, analytical errors). The activation energy of the sphene glass is certainly underestimated because of the protective effect observed at 200°C. An activation energy of 60 kJ mol^{-1} can be postulated for all these glasses; this value is within the range attributed to the surface-controlled silicate dissolution reactions (Lasaga, 1984).

4.2. Evolution of the alteration rate with increased reaction progress

In addition to their common initial rate, the three aluminosilicate glasses in this study—as well as tholeitic basalt glass and R7T7 nuclear glass—exhibit a similar reduction in the alteration rate as the reaction progresses. This behavior may be explained in two ways: by the formation of a surface alteration layer with protective properties, or due to saturation effects by thermodynamic equilibration of the pristine glass and solution through the definition of a glass solubility product.

4.2.1. Formation of a protective altered surface layer

The protective effect of a modified surface layer may be considered in various ways. It may constitute a diffusion barrier creating a concentration gradient near the reaction interface, or a screen in which its stability, with respect to the leachate, could control the alteration kinetics (Bourcier et al., 1990).

R7T7 glass alteration is accompanied by the formation of a surface gel (Vernaz and Dussossoy, 1992) that retains elements including those with oxides and hydroxides that are relatively insoluble in slightly basic media (pH 7–10); these include Al, Fe, Zr, the rare earth elements and the actinides. Dissolution of basaltic glass at high temperatures (> 150°C) results in the development of a residual hydrated gel (Berger et al., 1987). When the thickness of this layer increases or when its permeability decreases, the dissolution rate becomes controlled by the diffusion of aqueous species exchanged between the reaction interface (beneath the gel) and the bulk solution. The protective effect of such a layer is illustrated by experiments showing a drop in the dissolution rate with time, without any changes in the experimental conditions. The dissolution of sphene glass in flow-through conditions at 200°C (Fig. 2) is a typical example. The observation of a thick chemically and morphologically modified surface on the samples altered under these conditions supports this assumption. The characteristics of SiAlON glass dissolution

Table 9
Initial dissolution rates and activation energy of the sphene, zirconolite and SiAlON glasses compared with basaltic glass and R7T7 nuclear waste glass

Initial rates	Sphene	Zirconolite	SiAlON	Basalt	R7T7
mole Si m^{-2} s^{-1}					
90°C	2.76×10^{-8}	1.69×10^{-8}	3.41×10^{-8}		9.20×10^{-8}
150°C	4.37×10^{-7}	1.50×10^{-7}	2.83×10^{-7}	1.02×10^{-6}	1.49×10^{-6}
200°C	1.64×10^{-6}	2.45×10^{-6}	4.08×10^{-6}	7.59×10^{-6}	8.83×10^{-6}
g_{glass} m^{-2} d^{-1}					
90°C	0.35	0.21	0.55		1.06
150°C	5.57	1.91	4.54	9.67	17.16
200°C	20.89	31.13	65.48	130.64	101.72
Ea (kJ mol^{-1})	53 ± 5	63 ± 5	61 ± 5	64 ± 5	59 ± 5

in an open system can be viewed as a boundary case of this effect: the very low dissolution rates, and the strong effects of the stirring speed and SA/V ratio suggest that a remarkable protective effect occurs from the first few hours of the reaction. Given the high neodymium content of this glass, and the disappearance of the protective effect in sulfate solutions, we suspect that hydrolysis of Nd produces a sparingly soluble and very protective compound (hydroxide and hydroxicarbonate).

On the other hand, no surface layer was observed by SEM on all glass specimens altered in a closed system at 90°C at a high SA/V ratio in initially pure water, although under these conditions, the alteration rates dropped by four orders of magnitude compared with the initial rates. With SiAlON glass, however, a region of diminished electron contrast about 50 nm thick was observed at the glass/solution interface by TEM, and could correspond to an altered zone (Fig. 8). XPS analysis revealed chemical composition changes (notably Al enrichment relative to Si) in the first 10 nm at the outer surface of the grains altered in a closed system (Table 7). In other words, if the diminishing alteration rates are attributable to the development of a protective layer, then in this case, the layer must be extremely thin and yet highly protective. Such a modified layer can prevent alteration of the pristine glass in several ways: (1) dissolution of the modified layer is the limiting step of the overall reaction (Bourcier et al., 1990); the alteration progress then depends on the stability of this layer, and not of the pristine glass; and (2) glass dissolution occurs at the interface between the pristine glass and the modified layer, but the latter constitutes a diffusion barrier for the aqueous species exchanged between the glass and the solution, according to Berger et al. (1994).

The second assumption implies very low diffusion coefficients, given the thickness of the altered layer. As an example, the value of the diffusion coefficient of aqueous silica through the modified layer at 90°C was calculated from Eq. (4):

$$\frac{\mathrm{d}m}{S\mathrm{d}t} = D\frac{(C_1 - C_0)}{l} \tag{4}$$

where $\mathrm{d}m$ is the silica mass loss (g) from the pristine glass calculated from relative nitrogen release in the case of SiAlON glass, and where S, $\mathrm{d}t$, D, C_1, C_0 and l are the surface area (cm^2), time (s), diffusion coefficient ($cm^2\ s^{-1}$), Si concentrations on each face of the surface layer ($g\ cm^{-3}$), and layer thickness, respectively. Assuming a buffered Si concentration near the amorphous silica solubility limit in contact with the pristine glass (Berger et al., 1994), D was found to be on the order of 10^{-13} $cm^2\ s^{-1}$ for $l = 50$ nm. This value is intermediate between the typical diffusion coefficients of aqueous solutions (10^{-5} $cm^2\ s^{-1}$) and solid phases (10^{-17} $cm^2\ s^{-1}$).

Further investigation is necessary in this area to measure the diffusion coefficient during dedicated experiments using diffusion cells and silicon isotopic markers, and to compare the measured and calculated values. It is necessary to separate significant quantities of gel for this type of experimentation.

Finally, the formation of such protective surfaces could perhaps be explained by the presence of significant amounts of elements (including Zr, Ti and the rare earths) subject to condensation phenomena (olation or oxolation: Jolivet, 1994; Ricol, 1995).

4.2.2. Chemical affinity of the controlling reactions with respect to the fresh glass surface

The dependence between the dissolution rate and the leachate concentration cannot be ignored. The dependence of the silicate dissolution rate on the reaction affinity is widely debated in the literature and a general kinetic relation was proposed by several authors (Aagaard and Helgeson, 1982; Lasaga, 1984; Nagy et al., 1991; Berger et al., 1994; Oelkers and Schott, 1995):

$$r_d = k^+ \prod_j a_j^{m_j} f(\Delta G_r) = k^+ \prod_j a_j^{m_j}\left(1 - e^{\frac{\Delta G_r}{\sigma RT}}\right) \tag{5}$$

where k^+ (mol $cm^{-2}\ s^{-1}$) is the kinetic constant of dissolution and $f(\Delta G_r)$ is a function of the Gibbs free energy. The latter term accounts for the major variations in the alteration rate with the deviation from equilibrium, where $f(\Delta G_r = 0) = 0$. σ is a stoichiometric factor (≤ 1). It is often used as an adjustable parameter, in which its intrinsic value is highly empirical. For this reason, σ was assumed to be equal to 1.

For silicate glasses altered under near neutral or slightly basic conditions, Grambow (1985) and

Berger et al. (1994) emphasized the predominant role of the aqueous silica concentration. Other authors (Gin, 1996; Daux et al., 1997) recommend taking several oxide-forming elements (SiO_2, Al_2O_3 and Fe_2O_3) into account to calculate the apparent glass solubility. Advocat et al. (1998) suggest calculating a global solubility by taking all the oxide components (formers and modifiers) into account.

The closed-system dissolution rates at 90°C may exhibit the characteristics of a chemical affinity effect. This raises the question of the nature of the controlling reaction: Does the solution equilibrate with the sound glass? If this is the case, a solubility product must be defined for the glass together with a precise dissolution equation. Consider the following equations for sphene glass Eq. (6) and zirconolite glass Eq. (7):

$$\begin{aligned}&Si_{0.5028}Al_{0.1743}Ca_{0.2606}Ti_{0.1161}Nd_{0.0667}O_{1.8599}\\&\quad+0.9325H_2O+0.2308H^+\rightleftarrows 0.5028H_4SiO_4^0\\&\quad+0.1743Al(OH)_4^-+0.2606Ca^{2+}\\&\quad+0.1161Ti(OH)_5^-+0.0667Nd(OH)_3^0\end{aligned}\tag{6}$$

$$\begin{aligned}&Si_{0.4871}Al_{0.1690}Ca_{0.2525}Ti_{0.1125}Zr_{0.0495}Nd_{0.0278}O_{1.8459}\\&\quad+0.9973H_2O+0.1739H^+\rightleftarrows 0.4871H_4SiO_4^0\\&\quad+0.1690Al(OH)_4^-+0.2525Ca^{2+}\\&\quad+0.1125Ti(OH)_5^-+0.0495Zr(OH)_5^-\\&\quad+0.0278Nd(OH)_3^0\end{aligned}\tag{7}$$

The equilibrium relation between the leachate and the glass should then be defined as follows:

$$\frac{Q}{K_{eq}}=\exp\left(\frac{\Delta G_r}{RT}\right)\tag{8}$$

where Q is the ionic activity product, K_{eq} is the solubility product, ΔG_r is the Gibbs free energy of reaction, R is the ideal gas constant, and T is the absolute temperature. The chemical reaction affinity is then defined by the relation: $A=-\Delta G_r$.

At equilibrium, $\Delta G_r=0$ and K_{eq} may therefore be estimated directly from the alteration solution composition if the corresponding glass alteration rate is nil. In the present work, K_{eq} was estimated for sphene and zirconolite glasses at 90°C independently of the experimental leaching data, based on the solubility products K_i of the i oxide components of the respective glasses (Table 1) weighted according to their molar fractions x_i by applying the ideal solid solution relation:

$$\log K_{eq}=\sum_i x_i\log K_i+\sum_i x_i\log x_i\tag{9}$$

corresponding to a standard free energy of reaction:

$$\Delta G_r=\sum_i x_i\Delta G_{i,r}^0+RT\sum_i x_i\ln x_i\tag{10}$$

where $\Delta G_{i,r}^0$ represents the standard free energy of reaction for oxide i. Eq. (10) is similar to the relation proposed by Paul (1977) or by Jantzen and Plodinec (1984) except for the entropic mixing term $RT\sum x_i\ln x_i$. The solubility product K_{eq} of sphene glass is thus -1.76, compared with -0.44 for zirconolite glass.

The ionic activity products Q were next calculated from the dissolved species concentrations determined in the leachates at each time interval for each glass. The activities of the aqueous species (Si, Al and Ca) were calculated with the EQUIL(T) code (Fritz, 1981). The activities of the other aqueous species (Ti, Zr and Nd) were directly estimated from the concentrations (no ionic force corrections), by taking into account the dissociation constants reported by Allard and Beall (1978), Cox et al. (1989) and Wagman et al. (1982). The resulting Q values were then substituted in Eq. (8) to obtain ΔG_r for each experimental point. Finally, the calculated ΔG_r values can be used to test the kinetic relation Eq. (5), which can be simplified as follows:

$$r_d=r_0\left(1-e^{\frac{\Delta G_r}{RT}}\right)\tag{11}$$

where r_0 is the initial dissolution rate at a given temperature ($r_0=k^+[H^+]^{-n}$; in the present work, this dependence was not determined).

The dissolution rates for sphene and zirconolite glass are plotted in Fig. 10 vs. the expression $(1-e^{\Delta Gr/RT})$ for all of our experiments. The following observations may be made from the figure.

- For both the sphene and zirconolite glasses, the maximum alteration rates near 0.3 g m^{-2} d^{-1} are

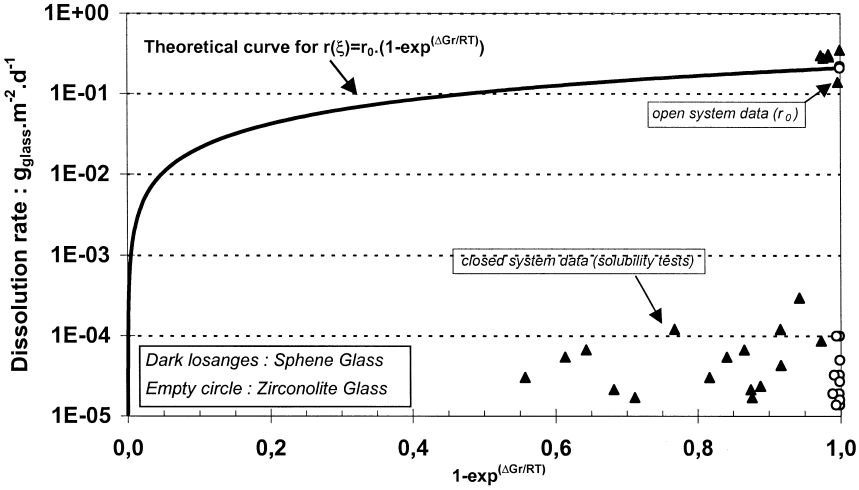

Fig. 10. Test of a kinetic relation between the instantaneous experimental dissolution rates at 90°C and the calculated global chemical affinity, for the sphene and zirconolite glass compositions.

associated with values near 1 for the $(1 - e^{\Delta Gr/RT})$ term; this is logical with very low leachate concentrations.

- The rates measured during sphene glass leach tests at 200 cm^{-1} ranged from 10^{-5} to 10^{-4} g m^{-2} d^{-1}. These low rates are associated with values around 0.5 for the $(1 - e^{\Delta Gr/RT})$ term. Qualitatively, the alteration rate of sphene glass diminishes as ΔG_r increases. Quantitatively, however, Eq. (11) is not validated: at 200 cm^{-1}, with a calculated value of $(1 - e^{\Delta Gr/RT}) = 0.56$, the glass alteration rate should theoretically be $r_0 \times 0.56 = 0.168$ g m^{-2} d^{-1}; the actual experimental value was 4.35×10^{-5} g m^{-2} d^{-1}, or about four orders of magnitude lower.
- For zirconolite glass, the $(1 - e^{\Delta Gr/RT})$ term was always near 1, and did not vary within the reaction progress range investigated. The chemical reaction affinity would thus apparently have no effect on the alteration rate of zirconolite glass if Eq. (11) is correct.

Assuming the K_{eq} values are correct, the experimentally observed drop in the alteration rate during the tests at 200 cm^{-1} would not be simply related to a reaction affinity calculated only on the basis of a deviation from equilibrium in the alteration solution. Moreover, it is not impossible that dissolved species such as silica could simply inhibit glass dissolution even when the leaching solutions are highly undersaturated with respect to the glass. This inhibiting effect of silica on the dissolution kinetics has been described for R7T7 borosilicate glass by Advocat et al. (1998).

At the present time, it is impossible to provide a definitive explanation for the decrease in the dissolution rate. Further progress in this area can be achieved only by measuring the diffusion coefficients of the gels that can form on the glass surface during alteration, and by confirming the log K values determined from an ideal solid solution model using calorimetric techniques. Recent data on simplified ternary glasses reveal significant differences between the values calculated using the model of Paul (1977) and those determined from thermochemical measurements (Linard et al., 1997). Finally, the hypothesis of a protective screen in which its inherent solubility could control the glass dissolution kinetics cannot be discounted. A silicate gel can develop on the glass surface when the solution is concentrated in both Si and Al; it results from a true chemical equilibrium with the solution, and can redissolve when the solution composition is modified. The reversible decrease in the zirconolite glass dissolution rate observed at 200°C during flow-through tests, as well as the slow rates and the solution composition in a closed system, can be attributed to the properties of such a thin protective silicate gel. This assumption implies that the composition and solubility product of such a protective layer must be known to allow

accurate prediction of long-term glass dissolution rates.

5. Conclusions

The dissolution of three aluminosilicate glasses with different compositions was investigated in open and closed systems. The initial dissolution rates were measured at 90, 150 and 200°C in open-system experiments with constant feeding of pristine solution. The initial rates were comparable for the three glass compositions, and were on the same order of magnitude as those previously measured with basaltic aluminosilicate glasses and aluminoborosilicate nuclear glasses. The activation energy determined from these data (60 ± 5 kJ mol^{-1}) is characteristic of a surface-controlled aluminosilicate dissolution reaction.

Additional open-system experiments conducted with lower renewal rates at 90 and 200°C showed a drop in the dissolution rates that could be related to the protective effects of alteration films on the glass surface. These effects differ according to the glass composition, and notably with regard to the nature and concentration of the network modifiers. SiAlON glass containing 53 wt.% Nd_2O_3 instantaneously develops a passivating layer that is prevented only by the existence of a neodymium complexing agent (e.g., sulfate) in solution. Zirconolite glass also develops an alteration surface, but it is less protective than the one observed on SiAlON glass. For sphene glass, a protective effect is observed only at high temperatures after several hours of alteration.

A final series of experiments was carried out in closed-system conditions at 90°C for 3 months at an SA/V ratio of 200 cm^{-1} to determine the dissolution rates at high reaction progress. Under these conditions, no significant amount of secondary phases were identified by conventional techniques (XRD, SEM, TEM), although the dissolution rates were very low (four orders of magnitude below the initial rates). In a closed system, these low rates may reflect either a low chemical affinity of glass dissolution, or the formation of a thin (< 50 nm), but protective silicate gel layer. Further progress in this area will require not only more comprehensive thermodynamic data (notably for ΔG_r^0), but also data on the diffusion coefficients of the gel that forms during alteration of the glass surface.

Acknowledgements

The authors would like to thank C. Fillet (CEA, Waste Containment Service) for the synthesis of the sphene and zirconolite glasses, and J. Rocherulle (University of Rennes) for the synthesis of the SiAlON glass. The authors would also like to thank D. Oquab and G. Chataignier (ENSCT) for their technical assistance with the SEM and XPS technics, and D. Beaufort for the TEM examinations. The manuscript has been greatly improved by the comments and suggestions of three reviewers: B. Bourcier, J.L. Crovisier and K.V. Ragnarsdottir. This work was funded by a CEA program 'Epac 6782-céramiques et vitrocristallins pour le confinement des radioéléments à vie longue'. *[SB]*

References

Aagaard, P., Helgeson, H.C., 1982. Thermodynamic and kinetic constraints on reaction rates among minerals and aqueous solutions: I. Theoretical considerations. Am. J. Sci. 282, 237–285.

Abrajano, T.A., Bates, J.K., Jr., Bradley, J.P., 1990. Analytical electron microscopy of leached nuclear waste glasses. In: Mellinger, G.B. (Ed.), Ceramic Transactions 9—Nuclear Waste Management III, pp. 211–228.

Advocat, T., 1991. Les mécanismes de corrosion en phase aqueuse du verre nucléaire R7T7. Approche expérimentale. Essai de modélisation thermodynamique et cinétique. PhD Thesis, Univ. Strasbourg, France, 229 pp.

Advocat, T., Crovisier, J.L., Dussossoy, J.L., Vernaz, E., 1993. Effects of MgO on the short and long-term stability of R7T7 nuclear waste glass in aqueous media. Sci. Basis Nucl. Waste Manage., Mater. Res. Soc. Symp. Proc. 294, 177–182.

Advocat, T., Chouchan, J.L., Crovisier, J.L., Guy, C., Daux, V., Jégou, C., Gin, S., Vernaz, E., 1998. Borosilicate nuclear waste glass alteration kinetics: chemical inhibition and affinity control. In: McKinley, I.G., McCombie, C. (Eds.), Sci. Basis Nucl. Waste Manage. XXI, Mater. Res. Soc. Symp. Proc, Vol. 506, pp. 63–70.

Allard, B., Beall, G.W., 1978. Predictions of actinide species in the groundwater. Workshop on the Environmental Chemistry and Research of the Actinides Elements, 8–12 October, Warrenton, VA, USA.

Berger, G., 1995. The dissolution rate of sanidine between 100 and 300°C. Water-Rock Interaction, Kharaka and Chudaev, Balkema, Rotterdam. ISBN 9054105496, pp. 141–144.

Berger, G., Schott, J., Loubet, M., 1987. Fundamental process controlling the first stage of alteration of a basalt glass by seawater: an experimental study between 200°C and 320°C. Earth Planet. Sci. Lett. 84, 431–445.

Berger, G., Schott, J., Guy, C., 1988. Behavior of Li, Rb and Cs during basalt glass and olivine dissolution and chlorites, smectites and zeolites precipitation from seawater: experimental investigation and modelization between 50°C and 300°C. Chem. Geol. 71, 297–312.

Berger, G., Claparols, C., Guy, C., Daux, V., 1994. Dissolution rate of a basalt glass in silica-rich solutions: implications for long-term alteration. Geochim. Cosmochim. Acta 58, 4875–4886.

Bourcier, W.L., Peiffer, D.W., Knauss, K.G., McKeegan, K.D., Smith, D.K., 1990. A kinetic model for borosilicate glass dissolution based on the dissolution affinity of a surface alteration layer. Mat. Res. Soc. Symp. Proc. 176, 209–216.

Bourcier, W.L., Knauss, K.G., Jackson, K.J., 1993. Aluminum hydrolysis constant to 250° from boehmite solubility measurements. Geochim. Cosmochim. Acta 57, 747–762.

Castet, S., Dandurand, J.L., Schott, J., Gout, R., 1993. Boehmite solubility and aqueous speciation in hydrothermal solutions (90–350°C): experimental study and modeling. Geochim. Cosmochim. Acta 57, 4869–4884.

Caurel, J., 1990. Altération hydrothermale du verre R7T7. Cinétiques de dissolution du verre à 150° et 250°C, rôle des phases néoformées. PhD Thesis, Univ. Poitiers, France, 71 pp.

Chase, M.W., Davies, C.A., Downey, J.R., Frurip, D.J., McDonald, R.A., Syverud, A.N., 1985. JANAF Thermochemical Tables, 3rd edn. J. Phys. Chem. Ref. Data 14, Suppl. 1.

Chou, L., Wollast, R., 1985. Steady-state kinetics and dissolution mechanisms of albite. Am. J. Sci. 285, 963–993.

Cox, J.D., Wagman, D.D., Medvedev, V.A., 1989. CODATA Key Values for Thermodynamics. Hemisphere Publishing, New York, 271 pp.

Crovisier, J.L., Fritz, B., Grambow, B., Eberhart, J.P., 1985. Dissolution of basaltic glass: experiments and thermodynamic modeling. In: Werme, L. (Ed.), Sci. Basis Nucl. Waste Manage, Mater. Res. Soc. Symp. Proc., 50, pp. 273–280.

Crovisier, J.L., Honnorez, J., Eberhart, J.P., 1987. Dissolution of basaltic glass in seawater: mechanism and rate. Geochim. Cosmochim. Acta 51, 2977–2990.

Daux, V., Guy, C., Advocat, T., Crovisier, J.L., Stille, P., 1997. Kinetic aspects of basaltic glass dissolution at 90°C: role of aqueous silicon and aluminium. Chem. Geol. 142, 109–126.

Delage, F., Dussossoy, J.L., 1991. R7T7 glass initial dissolution rate measurements using a high-temperature Soxhlet device. In: Teofilo, A., Abrajano, Jr., Johnson, L.H. (Eds.), Sci. Basis Nucl. Waste Manage. XIV, Mater. Res. Soc. Symp. Proc., pp. 41–47.

Dove, P., Crerar, D., 1990. Kinetics of quartz dissolution in electrolyte solutions using a hydrothermal mixed flow reactor. Geochim. Cosmochim. Acta 54, 955–969.

Fillet, S., 1987. Mécanismes de corrosion et comportement des actinides dans le verre nucléaire R7T7. PhD Thesis, Univ. Montpellier, France, 338 pp.

Fillet, C., Marillet, J., Dussossoy, J.L., Pacaud, F., Jacquet-Francillon, N., Phalippou, J., 1998. Titanite and zirconolite glass ceramics for long-lived actinide immobilization. In: Peeler, D.K., Marra, J.C. (Eds.), Environmental Issues and Waste Management Technologies in the Ceramic and Nuclear Industries III, Ceramic Transaction, Vol. 87. American Ceramic Society.

Fritz, B., 1981. Etude thermodynamique et modélisation des réactions hydrothermales et diagénétiques. Mémoire Sciences Géologique, ULP-Univ. L. Pasteur de Strasbourg, no. 65.

Gin, S., 1996. Control of R7T7 nuclear glass alteration kinetics under saturation conditions. Sci. Basis Nucl. Waste Manage., Mater. Res. Soc. Symp. Proc. 412, 189–196.

Grambow, B., 1985. A general rate equation for nuclear waste glass corrosion. Sci. Basis Nucl. Waste Manage., Mater. Res. Soc. Symp. Proc. 44, 15–21.

Grambow, B., 1987. JSS-A glass dissolution: mechanism, model and experiments. SKB Tech. Rept 87-02. Swedish Nuclear Fuel and Waste Management, Stockholm.

Guy, C., 1989. Mécanismes de dissolution des solides dans les solutions hydrothermales déduits du comportement de verres basaltiques et de calcites déformées. PhD Thesis, Univ. Toulouse, France, 188 pp.

Guy, C., Schott, J., 1989. Multisite surface reaction versus transport control during the hydrolysis of a complex oxide. Chem. Geol. 78, 181–204.

Holdren, G.R., Speyer, P.M., 1985. pH dependent changes in the rates and stoichiometry of dissolution of an alkali feldspar at room temperature. Am. J. Sci. 285, 994–1026.

Jantzen, C., Plodinec, M., 1984. Thermodynamic model of natural, medieval and nuclear waste glass durability. J. Non-Cryst. Solids 67.

Jolivet, J.P., 1994. De la solution à l'oxyde. InterEditions/CNRS Editions.

Jollivet, P., 1996. Modeling the lifetime of a high-level containment glass package under disposal conditions. Conf. Proc., Global '95, Versailles, France.

Lasaga, A.C., 1984. Chemical kinetics of water–rock interactions. J. Geophys. Res. 89, 4009–4025.

Leturcq, G., 1998. Alteration et Comportement à long terme de différentes classes de matériaux innovants pour le confinement des radionucléides à vie longue. Thèse de Doctorat de l'Université Paul Sabatier de Toulouse, 207 pp.

Leturcq, G., Berger, G., Advocat, T., Delage, F., Rocherulle, J., Vernaz, E., 1997. Chemical durability of a Nd doped oxynitride glass. Ceramic Transaction, American Ceramic Society Proceedings (1997—fall meeting, Cincinatti).

Linard, Y., Neuville, D.R., Richet, P., 1997. Thermochimie des verres de stockage de déchets nucléaires: une nouvelle approche. Le verre, Recherche scientifique pour un confinement de haute performance, Summer School Proceeding, CEA-Valrho, France, 31 August to 7 September (1997), pp. 362–373, 688 pp.

Lutze, W., Ewing, R., 1988. Radioactive Waste Forms for the Future. North-Holland Physics Publishing, Elsevier.

Ménard, O., 1995. Partage des terres rares et des actinides entre

solution et produits d'altération du verre nucléaire type R7T7 en fonction des conditions de stockage. PhD Thesis, Univ. Aix-Marseille III, France, 273 pp.

Ménard, O., Advocat, T., Ambrosi, J.P., Michard, A., 1998. Behaviour of actinides (Th, U, Np and Pu) and rare earths (La, Ce and Nd) during aqueous leaching of a nuclear glass under geological disposal conditions. Appl. Geochem. 13, 105–126.

Nagy, K.L., Blum, A., Lasaga, A., 1991. Dissolution and precipitation kinetics of kaolinite at 80°C and pH 3: dependence on solution saturation state. Am. J. Sci. 291.

Noguès, J.L., 1984. Les mécanismes de corrosion des verres de confinement des produits de fission. PhD Thesis, Univ. Montpellier, France, 322 pp.

Oelkers, E., Schott, J., 1995. Experimental study of anorthite dissolution and the relative mechanisms of feldspar hydrolysis. Geochim. Cosmochim. Acta 59, 5039–5053.

Paul, A., 1977. Chemical durability of glasses: a thermodynamic approach. J. Mater. Sci. 12, 2246–2268.

Phillips, S.L., Hale, F.V., Silvester, L.F. Siegel, M.D., 1988. Thermodynamic tables for nuclear waste isolation, an aqueous solutions database, Vol. 1, Report NUREG/CR-4864, LBL-22860, SAND87-0323. Lawrence Berkeley Laboratory, Berkeley, CA, USA, 181 pp.

Reimann, G.A., Kong, P.C., 1993. Improving iron-enriched basalt with additions of ZrO_2 and TiO_2, INEL report EGG-MS-10642, 30 pp.

Ricol, S., 1995. Etude du gel d'altération des verres nucléaires et synthèse de gels modèles. PhD Thesis, Univ. Paris, France, 177 pp.

Rocherullé, J., Verdier, P., Laurent, Y., 1989. Preparation and properties of gadolinium oxide and oxynitride glasses. Mater. Sci. Eng. B 2, 265–268.

Strickland, J.D.H., Parksons, T.R., 1972. Determination of reactive silicate. A Practical Handbook of Seawater Analysis, Fisheries Research Board of Canada Bull. 61, pp. 65–70.

Tovena, I., 1995. Influence de la composition des verres nucléaires sur leur altérabilité. PhD Thesis, Univ. Montpellier, France, 401 pp.

Trotignon, L., 1990. La corrosion des verres borosilicatés: nature et propriétés des couches d'altération. PhD Thesis, Univ. Toulouse, France, 161 pp.

Vernaz, E., Dussossoy, J.L., 1992. Current state of knowledge of nuclear waste glass corrosion mechanisms: the case of R7T7 glass. Appl. Geochem., Suppl. Issue no. 1, 13–22.

Wagman, D.D., Evans, W.H., Parker, V.B., Schumm, R.H., Halow, I., Bailey, S.M., Churney, K.L., Nuttall, R.L., 1982. The NBS tables of chemical thermodynamic properties: selected values for inorganic and C1 and C2 organic substances in SI units. J. Phys. Chem. Ref. Data 11, 1–392, Suppl. 2.

Zachariasen, W.H., 1932. The atomic arrangement in glass. J. Am. Ceram. Soc. 54, 3841–3851.